horticulturae

MDPI

Article

Genome-Wide Identification and Expression Pattern Analysis of the *Stewartia gemmata WRKY* Gene Family Within an Evolutionary Framework

Xiaohan Yuan, Zhehui Zhu, Fan Wang, Jieyu Lin, Syeda Hamna and Hanyang Lin *

Zhejiang Key Laboratory for Restoration of Damaged Coastal Ecosystems, School of Life Sciences, Taizhou University, Taizhou 318000, China
* Correspondence: hylin@tzc.edu.cn

Abstract

WRKY is one of the major transcription factor (TF) families in plants and is involved in various biological processes. However, studies on WRKY TFs are lacking in *Stewartia*, an early-diverged genus of Theaceae. This study aims to identify and analyze the WRKY members in *S. gemmata*, a deciduous tree with horticultural potential. We predicted their potential roles and explored their evolutionary relationships with those in other Theaceae species. Our study identified 87 *WRKY* genes in *S. gemmata*, which were classified into three groups (group I, II, and III). Groups I and II-c contained the most *SgWRKY* genes, a pattern consistently found in the other four *Camellia* species examined, providing a basis for further investigation into the potential roles of these genes in functioning. In addition, we revealed gene expression patterns in leaves and floral organs with qRT-PCR validation, identifying four *SgWRKY* genes (*SgWRKY24*, *SgWRKY84*, *SgWRKY67*, and *SgWRKY77*) that were upregulated in multiple comparisons across flowering stages. Collinearity and selection pressure analyses further supported sequence conservation and the presence of purifying selection among analyzed gene pairs. *Cis*-acting element prediction and enrichment analyses also suggested that these four *SgWRKY*s may play roles in plant development, stress responses, and secondary metabolism regulation. Collectively, our findings lay the foundation for further functional genomics of *SgWRKY* genes and provide insights into the evolution of WRKY TFs in Theaceae.

Keywords: WRKY transcription factors; *Stewartia gemmata*; flowering stages; phylogenetic analysis; gene expression patterns; synteny analysis

Check for updates

Academic Editor: David P. Horvath

Received: 8 September 2026
Revised: 21 October 2026
Accepted: 23 October 2026
Published: 25 October 2026

Copyright: © 2026 by the authors. Licensee MDPI, Basel, Switzerland. This article is an open access article distributed under the terms and conditions of the Creative Commons Attribution (CC BY) license.

1. Introduction

Transcription factors (TFs) are DNA-binding proteins that recognize specific nucleotide sequences to modulate the transcription of target genes, playing crucial roles in diverse biological processes [1,2]. WRKY represents one of the largest plant TF families [3,4] and is not only involved in plant development and the response to environmental stresses but also regulates the biosynthesis of secondary metabolites [5–12]. Members of this family are characterized by their conserved WRKYGQK motif and zinc-finger structures, both of which enable sequence-specific DNA binding to W-boxes *cis*-elements (TTGAC(C/T)) [3,4]. Based on the number of WRKY domains and the features of their zinc-finger motifs, WRKY TFs can be classified into three groups (I, II, III) [3,4]. Group II can be further divided into five subgroups (II-a, II-b, II-c, II-d, and II-e) according to their phylogenetic relationships [3,4,13].

There are two WRKY domains included in group I, while group II and group III contain only one. Group I and group II share the same zinc finger (C-$X_{4–5}$-C-$X_{22–23}$-H-X-H [C_2H_2]), whereas group III contains a distinct zinc-finger motif (C-X_7-C-X_{23}-H-X-C [C_2HC]) [3,4]. The first cDNA encoding a WRKY protein named SPF1 was cloned from sweet potato (*Ipomoea batatas*) in 1994 but was not commonly found in other species at that time [14]. With the rapid advancement of genomic research, an expanding array of *WRKY* genes has been identified across diverse plant species. Evidence suggests that the higher number of *WRKY* genes in plants may reflect lineage-specific gene duplication and retention, which can provide genetic material for functional innovation, such as enhanced adaptive potential to extreme environments [15], whereas the lower number of *WRKY* genes may result from genomic structural variation [16].

Stewartia (Theaceae) is recognized as the earliest-diverged clade within the tea family [17,18], comprising approximately 20 species [19]. Unlike predominantly evergreen genera such as *Camellia*, *Stewartia* is the only genus that contains extant deciduous species, providing a valuable research direction to investigate the factors underlying its deciduous habit. *Stewartia gemmata* was first described in 1931 based on type material collected from Mt. Tianmu in Zhejiang Province [20], which is deciduous mainly distributed in southeastern China [21,22]. Species in the tea family hold significant economic and ecological importance, including *Camellia sinensis*, the source of tea, as well as ornamental species [23] and timber-producing trees [24]. Additionally, many plants in this family have strong environmental adaptability and high ecological plasticity [25,26], playing indispensable roles in maintaining natural ecosystems. *S. gemmata* harbors prominent horticultural potential. The tree is distinguished by its grayish-yellow to brownish bark, which peels away in thin flakes to reveal the mottled surface, and its white flowers with yellow stamens are delicate and attractive, rendering it a valuable landscape tree suitable for street planting and garden ornamentation [19,27]. Given the roles of WRKY TFs in plant development, studying WRKY TFs in *S. gemmata* may not only help explain its deciduous habit but also provide new insights into the improvement of horticultural traits. Moreover, this species represents a good candidate for investigating the comparative evolutionary history of gene families within the tea family [17,28,29], as supported by genomic data and fossil evidence.

Previous studies have demonstrated the molecular mechanisms by which WRKY TFs function in *Camellia sinensis*. For example, overexpression of *CsWRKY7* resulted in a late-flowering phenotype under normal growth conditions [30]. CsWRKY71 regulated the synthesis of theanine in tea plants in response to exogenous gibberellin treatment [31]. CsWRKY17 promoted pectin de-esterification by binding to the *CsPME6* promoter to enhance aluminum accumulation [32]. In addition, Chen et al. (2025) reported that *CsWRKY51*-overexpressing plants exhibited dwarfism, curled leaves, increased branching, and enhanced flowering, along with significantly elevated accumulation levels of amino acids, including glutamine, asparagine, and arginine [33]. However, the *WRKY* gene family in *S. gemmata* remains uncharacterized, and whether it shares the composition and evolutionary patterns observed in *Camellia* remains to be examined.

By leveraging high-quality genome assemblies, we conducted a genome-wide identification and characterization of *WRKY* genes in *S. gemmata* and compared them with those in four *Camellia* species. Specifically, we combined phylogenetic, gene duplication, synteny, and selective pressure analyses to examine family composition and sequence conservation, and used RNA-seq and qRT-PCR to characterize expression patterns in leaves and floral organs across three flowering stages. These analyses aimed to clarify the evolutionary characteristics of the WRKY TF family in *S. gemmata* and identify candidate genes for subsequent functional investigation. These findings provide a resource for future functional

genomics research and may facilitate future efforts to improve the horticultural value of *S. gemmata*.

2. Materials and Methods

2.1. Identification of WRKY Gene Family Members in Stewartia gemmata and Four Other Species in Theaceae

The WRKY protein sequences of *Arabidopsis thaliana* were downloaded from the Arabidopsis Information Resource website (TAIR, http://www.arabidopsis.org/, accessed on 11 February 2025) [34]. Then, we acquired the Hidden Markov Model (HMM) file of the WRKY domain (PF03106) from the Pfam database (v. 36.0) (http://pfam.xfam.org/, accessed on 11 February 2025) [35]. The *S. gemmata* reference genome and its annotation were generated by our group as part of an unpublished study (https://doi.org/10.6084/m9.figshare.28356032). The genome was assembled based on PacBio SMRT HiFi data and Hi-C reads and annotated by combining homology-based inference, ab initio prediction, and RNA-seq transcript assemblies. The final assembled genome was 2.87 Gb in size and of good quality, with a contig N50 of 17.43 Mb, 97.7% complete BUSCOs, and a long terminal repeat assembly index (LAI) of 17.45. A total of 45,436 protein-coding genes were predicted. Subsequently, we searched the WRKY sequences in the *S. gemmata* genome using the BLAST program (v. 2.12.0; a cutoff of $E \leq 1 \times 10^{-5}$) and the Simple HMM Search program available from TBtools (v. 2.064) [36]. Finally, we removed duplicate results and retained the intersection of the outputs of the two methods, which were considered candidate SgWRKY TFs. The candidate WRKY TFs of *Camellia chekiangoleosa* [37], *Camellia lanceoleosa* [38], *Camellia oleifera* [39], and *Camellia sinensis* [40] were identified using the same methods.

2.2. Physicochemical Properties Analysis of SgWRKY TFs

The Online Tool ExPASy [41] and the WoLF PSORT tool [42] were used to analyze the physicochemical properties and the subcellular localization information of the SgWRKY TFs. We applied TargetP-2.0 to predict the presence of targeted proteins [43]. Furthermore, the nuclear localization signal (NLS) motifs were predicted by the NLStradamus tool [44].

2.3. Chromosomal Location, Gene Duplication, and Collinearity Analysis of SgWRKY Genes

The genomic positions of *SgWRKY* genes and the lengths of each chromosome were obtained from the genome sequence and annotation files using TBtools. MCScanX [45] available from TBtools (E-value cutoff: 1×10^{-5}) was used to investigate gene duplication events within *S. gemmata* and the similarity of *SgWRKY* genes between *S. gemmata* and five other species (*C. chekiangoleosa*, *C. lanceoleosa*, *C. oleifera*, *C. sinensis*, and *A. thaliana*). Non-synonymous (*Ka*) and synonymous (*Ks*) substitution rates were estimated using DnaSP (v. 6.12.03) [46] after multiple sequence alignment with the MUSCLE algorithm implemented in MEGA12 (v. 12.0.9) [47].

2.4. Conserved Motifs, Cis-Acting Elements, and Gene Ontology Analysis of SgWRKY Genes

87 SgWRKY TFs were submitted to the NCBI CDD database [48] and the Batch SMART program in TBtools for validation of conserved domains. As for conserved motifs, we used the Clustal Omega program (v. 1.2.4) available from the EMBL-EBI Job Dispatcher to align the sequences [49], which were later visually compared with the Jalview program (v. 2.11.5.2) [50]. The WebLogo tool (v. 2.8.2) [51] was used to visualize the sequences of the conserved SgWRKY motifs. The MEME suite tool (v. 5.5.7) [52] was also used to perform conserved motif analysis, and the motif number was set to 10. Meanwhile, the neighbor-joining (NJ) tree of SgWRKY proteins was inferred using MEGA12 and then visualized using tvBOT (v. 2.6.1) [53]. In addition, we applied the PlantCARE database [54]

to search for *cis*-acting regulatory elements (2000 bp upstream of the start codon) of *SgWRKY* genes for gene structure analysis. Next, Gene Ontology (GO) annotation and enrichment analyses were performed using homology searches against the *A. thaliana* genome using KOBAS-i [55]. We focused specifically on the 'biological process' GO category, retaining only terms with a significance threshold of p-value < 0.05 (Fisher's exact test with Benjamini–Hochberg correction).

2.5. Phylogenetic Tree Analysis

We utilized MAFFT (v. 7.508; --auto) [56] to align the WRKY protein sequences of six different species (*S. gemmata*, *A. thaliana*, *C. sinensis*, *C. chekiangoleosa*, *C. lanceoleosa*, and *C. oleifera*). Then, we used trimAl (v. 1.4;--automated1) [57] to trim the alignment. Later, IQ-TREE (v. 2.2.0.3) [58] was used to infer the maximum likelihood (ML) phylogenetic tree with 1000 ultra-fast bootstrap (BS) replicates [59]. The best-fit protein substitution model was determined automatically with ModelFinder, as supported by IQ-TREE (-m MFP) [60], and JTT+F+I+R6 was inferred to be the best model.

2.6. Sample Collection and Transcriptome Sequencing

To explore the gene expression patterns during flowering stages, we collected a total of 27 leaf and 27 floral organ samples from *S. gemmata* at three stages (S1: 10:00 AM, 12 April 2025; S2: 10:00 AM, 26 April 2025; S3: 10:00 AM, 17 May 2025; all sunny days) with increasing temperature (S1: 18 °C; S2: 24 °C; S3: 28 °C) in Hangzhou Botanical Garden (HZBG), Zhejiang Province. These three sampling stages corresponded to progressive floral development. In S1 and S2, we collected flower buds, while in S3, blooming flower organs were sampled. Three biological replicates for each stage were sampled. The three sampled trees are of the same age and growth condition and were all germinated from seeds sampled on Mt. Tianmu (where the type specimen of *S. gemmata* was collected) in the 1950s (personal communication from HZBG). Samples were liquid-nitrogen frozen at HZBG and stored at −80 °C until use. RNA extraction and transcriptome sequencing were performed at a commercial sequencing institute following standard protocols (Annoroad Gene Technology Co., Ltd., Beijing, China). The purity, concentration, and integrity of RNA products were evaluated on a NanoDrop 2000 microspectrophotometer and a LabChip GX Touch microfluidic capillary system. RNA samples were considered qualified when they exhibited an OD260/OD280 ratio of ca. 2.0, total RNA amount above 1 µg, and RNA integrity number (RIN) > 6 [61]. Raw sequencing reads were processed to remove adapter sequences, reads containing ambiguous bases, and low-quality reads ($Q \leq 20$ bases accounted for more than 50% of the entire read length). The filtering process was performed using in-house scripts developed by the sequencing institute, and the clean data for each sample were obtained (Table S1).

2.7. Expression Pattern Analysis of SgWRKY Genes

After quality control, clean transcriptomic reads were aligned to the *S. gemmata* genome using HISAT2 (v. 2.2.1) [62]. Gene expression quantification was performed using StringTie (v. 2.2.1) [63], and the read counts were obtained using the prepDE.py script (Table S2). Meanwhile, we implemented the getTPM.py script to normalize the read counts by gene length, producing the transcripts per kilobase per million mapped reads (TPM) profile. Subsequently, we used the R package DESeq2 (v. 1.44.0) [64] to identify differentially expressed genes (DEGs) from the read count matrices, with significance defined as $|\log_2$ fold-change ($\log_2$FC)$| > 1$ and adjusted p-value < 0.05. To investigate the temporal expression patterns of tissue-specific DEGs, complementary volcano plots and TPM heatmaps were generated using the ggplot2 package (v. 3.5.2) in R [65] and the RNAdiff module

(v 1.1.0) (https://github.com/nongxinshengxin/RNAdiffAPP, accessed on 20 July 2025) available from TBtools.

2.8. Quantitative Real-Time PCR (qRT-PCR) Analysis

Using mRNA as the template, we employed the SYBR Green dye-based approach [66] to conduct reverse transcription quantitative real-time PCR (qRT-PCR). We employed the FastKing RT Kit (with gDNase; TIANGEN Biotech, Co., Ltd., Beijing, China) to remove genomic DNA and synthesize cDNA. The *Csactin* gene was used as the internal reference [67,68]. The putative homolog of this gene in *S. gemmata* (transfrag09318) showed no significant differential expression across treatment comparisons in our RNA-seq data. Primers were designed with Primer3Web (v. 4.1.0) (Table S3) [69,70]. The qRT-PCR assays were performed using the ChamQ Universal SYBR qPCR Master Mix (Vazyme Biotech, Co., Ltd., Nanjing, China) on a CFX96^{TM} Real-Time PCR System (Bio-Rad Laboratories, Inc., Hercules, CA, USA) under the following conditions: initial denaturation at 95 °C for 1 min, followed by 40 cycles of 95 °C for 5 s and 60 °C for 30 s (annealing/extension). A melting curve analysis was subsequently performed to validate the specificity of the qPCR reactions. Relative expression levels were calculated using the $2^{-\triangle\triangle Ct}$ method [71] for gene expression quantification, with the levels in S1 serving as the reference. Finally, statistical comparisons of gene expression levels across the three flowering stages were performed using one-way analysis of variance (ANOVA) followed by Tukey's post-hoc test using the R package stats.

3. Results

3.1. Identification and Characterization of Members of the WRKY Protein Family

A total of 87 WRKY TFs were identified, all of which were verified to contain the WRKY domains by the NCBI CDD database (Table S4) and the SMART program (Table S5). These genes were renamed systematically from *SgWRKY1* to *SgWRKY87* based on the physical locations on the chromosomes. Moreover, a total of 90, 101, 99, and 93 WRKY proteins were identified in *Camellia chekiangoleosa*, *Camellia lanceoleosa*, *Camellia oleifera*, and *Camellia sinensis*, respectively.

The physicochemical properties of 87 SgWRKY proteins are shown in Table 1. The length of the amino acid sequences varied from 162 to 758 amino acids, with predicted molecular weights ranging from 18.377 to 82.468 kDa. The theoretical isoelectric points (pI) ranged from 4.7 to 9.96. Among these proteins, 53 had a pI below 7, 33 above 7, and one at exactly 7, indicating that the majority of them were acidic. According to the instability index (II) analysis, only two proteins (SgWRKY11, SgWRKY47) were predicted to be stable (index < 40), while the majority were classified as unstable (index > 40). The aliphatic index of the identified proteins ranged from 39.55 to 76.04 with an average value of 58.13. The hydrophilicity values of all proteins are negative. In addition, the NLS prediction analysis revealed that 9 out of the 87 proteins contained an NLS structure. Subcellular localization analysis suggested that SgWRKY39 and SgWRKY58 were localized to the peroxisome, while SgWRKY64 localized to the cytoplasm. Finally, all SgWRKY proteins were considered to lack targeting peptides.

Table 1. Physicochemical properties of 87 SgWRKY proteins.

Gene Name	Gene ID	Amino Acids	Molecular Weight (Da)	Isoelectric Point (pI)	Instability Index (II)	Aliphatic Index	Grand Average of Hydropathicity	Subcellular Localization	Targeting Protein	NLS
SgWRKY1	augustus55263.t01	171	19,294.72	9.60	46.38	54.04	−0.836	nucl	no	yes
SgWRKY2	augustus55266.t01	171	19,349.80	9.60	46.38	55.15	−0.838	nucl	no	yes
SgWRKY3	augustus55275.t01	171	19,402.86	9.44	47.48	56.32	−0.777	nucl	no	yes
SgWRKY4	augustus55276.t01	176	20,029.54	9.32	46.14	56.93	−0.802	nucl	no	yes
SgWRKY5	transfrag17078.t01	514	56,332.77	7.29	50.32	66.95	−0.695	nucl	no	no
SgWRKY6	transfrag17470.t01	346	38,323.34	9.62	56.87	66.53	−0.689	nucl	no	no
SgWRKY7	augustus72272.t01	189	21,418.51	6.66	50.98	43.23	−1.117	nucl	no	no
SgWRKY8	transfrag20504.t01	230	25,801.05	9.19	57.52	55.09	−0.710	nucl	no	no
SgWRKY9	transfrag34611.t01	528	57,382.15	7.32	59.26	51.80	−0.886	nucl	no	no
SgWRKY10	transfrag34627.t01	313	34,193.65	5.64	53.15	52.33	−0.818	nucl	no	no
SgWRKY11	augustus14889.t01	183	20,771.31	9.54	37.86	48.96	−0.891	nucl	no	yes
SgWRKY12	augustus12158.t01	684	73,558.28	5.76	53.89	58.80	−0.711	nucl	no	no
SgWRKY13	augustus10112.t01	616	67,126.21	6.30	49.61	61.88	−0.704	nucl	no	no
SgWRKY14	augustus10209.t01	472	51,999.38	8.85	57.66	66.00	−0.612	nucl	no	no
SgWRKY15	transfrag19646.t01	498	55,243.66	6.75	50.21	61.00	−1.014	nucl	no	no
SgWRKY16	transfrag19581.t01	620	67,381.81	6.24	52.77	59.55	−0.723	nucl	no	no
SgWRKY17	augustus09348.t01	430	46,924.03	5.59	68.14	71.21	−0.713	nucl	no	no
SgWRKY18	transfrag20750.t01	341	38,175.44	5.83	41.79	64.93	−0.760	nucl	no	no
SgWRKY19	transfrag20803.t01	570	63,130.77	6.82	57.50	42.46	−0.944	nucl	no	no
SgWRKY20	transfrag04540.t01	307	34,128.92	5.62	57.95	62.90	−0.686	nucl	no	no
SgWRKY21	transfrag04449.t01	479	52,137.61	8.61	43.22	57.20	−0.881	nucl	no	no
SgWRKY22	transfrag24377.t01	523	56,803.83	8.47	54.54	53.19	−0.777	nucl	no	no
SgWRKY23	augustus59867.t01	328	36,003.32	8.75	41.71	68.69	−0.684	nucl	no	no
SgWRKY24	transfrag27176.t01	307	34,289.27	6.61	46.56	66.32	−0.709	nucl	no	no
SgWRKY25	transfrag27177.t01	311	34,845.97	6.61	45.61	64.86	−0.754	nucl	no	no
SgWRKY26	transfrag27178.t01	286	31,953.88	8.34	45.48	63.71	−0.720	nucl	no	no
SgWRKY27	augustus51264.t01	420	47,213.53	5.29	63.33	50.81	−0.959	nucl	no	no
SgWRKY28	augustus51292.t01	317	34,543.05	9.65	49.91	60.95	−0.671	nucl	no	no
SgWRKY29	augustus45500.t01	184	20,710.58	5.57	55.99	49.89	−1.007	nucl	no	no
SgWRKY30	transfrag07950.t01	345	39,180.41	5.27	48.92	62.70	−0.747	nucl	no	no
SgWRKY31	transfrag32900.t01	332	36,722.91	7.00	44.36	65.51	−0.773	nucl	no	no
SgWRKY32	transfrag33314.t01	554	59,960.31	6.73	46.00	56.53	−0.722	nucl	no	no
SgWRKY33	transfrag18516.t01	528	57,294.38	5.42	62.53	63.01	−0.763	nucl	no	no
SgWRKY34	transfrag38014.t01	585	63,938.89	8.44	68.38	49.74	−0.898	nucl	no	no
SgWRKY35	transfrag28387.t01	345	38,892.05	9.73	50.16	62.46	−0.839	nucl	no	no
SgWRKY36	augustus49562.t01	266	30,227.09	4.82	67.00	52.41	−1.017	nucl	no	no
SgWRKY37	transfrag26280.t01	301	33,567.39	6.32	64.33	63.49	−0.718	nucl	no	no
SgWRKY38	transfrag15135.t01	348	38,874.79	5.58	53.17	55.78	−0.758	nucl	no	no
SgWRKY39	augustus28947.t01	208	23,149.39	9.59	56.28	70.29	−0.653	pero	no	no
SgWRKY40	transfrag15074.t01	336	37,266.35	4.91	54.62	60.39	−0.620	nucl	no	no
SgWRKY41	transfrag15073.t01	334	37,083.14	4.96	61.26	56.38	−0.638	nucl	no	no
SgWRKY42	transfrag15072.t01	350	39,108.13	4.70	59.41	57.69	−0.699	nucl	no	no
SgWRKY43	transfrag11401.t01	319	35,614.24	6.67	47.41	75.49	−0.515	nucl	no	no
SgWRKY44	augustus21817.t01	214	23,807.74	9.12	46.21	66.07	−0.670	nucl	no	no
SgWRKY45	transfrag21973.t01	331	36,201.19	9.47	50.42	76.04	−0.451	nucl	no	no
SgWRKY46	transfrag01099.t01	522	57,054.50	6.68	59.39	64.62	−0.685	nucl	no	no
SgWRKY47	transfrag31878.t01	162	18,377.75	9.60	35.36	57.04	−0.701	nucl	no	no
SgWRKY48	transfrag35729.t01	451	49,167.38	5.51	55.20	54.70	−0.714	nucl	no	no
SgWRKY49	augustus27943.t01	280	30,758.09	5.78	59.30	46.64	−0.807	nucl	no	yes
SgWRKY50	transfrag35066.t01	585	63,906.16	7.71	45.12	58.44	−0.662	nucl	no	no
SgWRKY51	transfrag29945.t01	333	36,881.75	5.89	67.46	39.55	−0.898	nucl	no	yes
SgWRKY52	augustus55969.t01	270	30,505.42	6.03	58.42	44.74	−1.054	nucl	no	no
SgWRKY53	transfrag13022.t01	600	65,362.38	6.39	47.29	53.57	−0.778	nucl	no	no
SgWRKY54	transfrag37226.t01	287	32,165.36	5.37	61.59	52.65	−0.840	nucl	no	no
SgWRKY55	augustus03409.t01	486	53,019.86	5.83	50.31	66.28	−0.733	nucl	no	no
SgWRKY56	transfrag15323.t01	221	25,218.62	7.68	50.07	44.48	−1.104	nucl	no	no
SgWRKY57	transfrag22300.t01	318	34,603.50	5.46	63.55	50.31	−0.722	nucl	no	no
SgWRKY58	augustus42329.t01	218	24,343.43	9.68	48.90	55.50	−0.864	pero	no	no
SgWRKY59	transfrag22411.t01	359	40,524.30	4.82	60.88	71.11	−0.596	nucl	no	no
SgWRKY60	augustus69412.t01	213	23,979.66	5.53	66.37	54.93	−0.987	nucl	no	yes
SgWRKY61	transfrag12218.t01	602	65,298.4	5.95	41.17	64.95	−0.633	nucl	no	no
SgWRKY62	transfrag12292.t01	486	53,771.29	7.02	45.70	59.07	−1.064	nucl	no	no
SgWRKY63	transfrag18794.t01	620	67,428.67	6.45	52.26	65.85	−0.611	nucl	no	no
SgWRKY64	augustus67317.t01	325	36,680.47	5.19	55.69	73.26	−0.521	cyto	no	no
SgWRKY65	augustus67316.t01	272	30,311.91	5.25	81.91	47.68	−0.790	nucl	no	no
SgWRKY66	transfrag21438.t01	251	28,526.47	5.21	61.62	51.27	−1.029	nucl	no	no
SgWRKY67	augustus40861.t01	280	31,629.54	5.88	60.98	55.71	−0.734	nucl	no	no
SgWRKY68	augustus05790.t01	294	32,958.37	9.96	51.09	69.63	−0.720	nucl	no	no
SgWRKY69	augustus05053.t01	578	63,869.73	7.70	62.01	46.06	−0.941	nucl	no	no
SgWRKY70	transfrag19491.t01	217	24,692.59	8.12	67.89	48.02	−0.840	nucl	no	no
SgWRKY71	transfrag30379.t01	346	38,333.98	9.43	45.58	55.29	−0.801	nucl	no	no
SgWRKY72	transfrag02522.t01	356	40,290.84	4.98	56.80	67.11	−0.679	nucl	no	no
SgWRKY73	augustus04712.t01	340	36,750.63	5.07	57.94	53.15	−0.664	nucl	no	no
SgWRKY74	transfrag30854.t01	219	24,627.99	7.65	52.11	42.69	−1.013	nucl	no	no
SgWRKY75	augustus10649.t01	347	39,624.87	9.75	61.92	62.33	−0.844	nucl	no	no
SgWRKY76	transfrag26486.t01	309	33,889.17	5.14	64.78	49.22	−0.890	nucl	no	no
SgWRKY77	transfrag26463.t01	532	57,715.68	7.69	59.63	52.11	−0.870	nucl	no	no
SgWRKY78	transfrag37437.t01	183	20,621.33	9.62	41.86	58.52	−0.807	nucl	no	yes
SgWRKY79	augustus09016.t01	758	82,468.96	5.86	55.37	55.20	−0.703	nucl	no	no

Table 1. *Cont.*

Gene Name	Gene ID	Amino Acids	Molecular Weight (Da)	Isoelectric Point (pI)	Instability Index (II)	Aliphatic Index	Grand Average of Hydropathicity	Subcellular Localization	Targeting Protein	NLS
SgWRKY80	transfrag37777.t01	319	35,795.91	4.96	75.91	64.76	−0.683	nucl	no	no
SgWRKY81	augustus70736.t01	210	22,748.52	6.84	51.49	65.95	−0.621	nucl	no	no
SgWRKY82	transfrag34191.t01	393	42,448.47	5.43	69.39	51.70	−0.734	nucl	no	no
SgWRKY83	transfrag34229.t01	371	40,955.23	5.74	45.98	56.82	−0.698	nucl	no	no
SgWRKY84	augustus66920.t01	333	37,185.15	6.18	47.84	60.93	−0.707	nucl	no	no
SgWRKY85	transfrag08701.t01	365	40,616.64	5.46	52.94	58.00	−0.795	nucl	no	no
SgWRKY86	transfrag09103.t01	296	33,809.77	5.33	61.48	66.49	−0.720	nucl	no	no
SgWRKY87	augustus16620.t01	404	43,601.71	6.76	57.61	55.74	−0.605	nucl	no	no

Footnote: Nucl stands for nucleus, pero for peroxisome, and cyto for cytoplasm.

3.2. Chromosomal Localization, Collinearity, and Selection Pressure Analysis of SgWRKY Genes

The 87 *SgWRKY* genes were unevenly distributed on the 17 chromosomes (Figure 1). Chromosome 1 harbored the highest number of *SgWRKY*s (11), followed by chromosome 6 with 10, while chromosome 16 contained the fewest, with only one *SgWRKY*. In addition, gene clusters were observed in the distal regions of chromosomes 1, 4, 6, 8, and 10 and near the centromeric regions of chromosomes 15 and 17. Collinearity analysis identified 57 segmental duplications of *WRKY* gene pairs and 8 tandem duplications of *WRKY* gene pairs (Figure 1, Table S6). The selective pressures on duplicated gene pairs were evaluated by calculating the *Ka*/*Ks* ratios (Table S6). Among the calculated results, 46 pairs had a $Ka/Ks < 1$ and 5 pairs had a $Ka/Ks > 1$, suggesting that most *SgWRKY* genes were under purifying selection pressure.

3.3. Conserved Motifs Analysis

WebLogo analysis of 87 SgWRKY protein sequences revealed the highly conserved heptapeptide (WRKYGQK) and the zinc-finger motifs (C_2H_2 or C_2HC) (Figure S1). However, some sequence variations were observed using Jalview (Figure 2). Specifically, this motif was WRKYGKK in SgWRKY7, SgWRKY29, and SgWRKY70, while it was WRKYGHK in SgWRKY3 and WRKYGRK in SgWRKY27. However, 8 SgWRKY proteins (SgWRKY12, SgWRKY17, SgWRKY49, SgWRKY60, SgWRKY64, SgWRKY65, SgWRKY68, SgWRKY81) were predicted to lack the zinc-finger motif. In addition, a total of 10 conserved motifs were found using the MEME tool (Figure S2) and visualized on the NJ tree (Figure S3). The number of observed motifs in each WRKY protein ranged from 2 to 6. In motif analysis, we found that motif 1 and motif 3 contain the highly conserved WRKYGQK domain, while motif 2 and motif 5 contain the zinc-finger structure. In addition, we also found that almost every WRKY protein contained motif 1 and motif 2. Notably, none of the group III members contained motif 5, and all group I members contained motif 3 except SgWRKY12. Furthermore, we observed that several motifs were specific to only one group: motif 8 and motif 3 were exclusive to group I, motif 9 to group II-d, and motif 10 to group II-c (found in SgWRKY1-4).

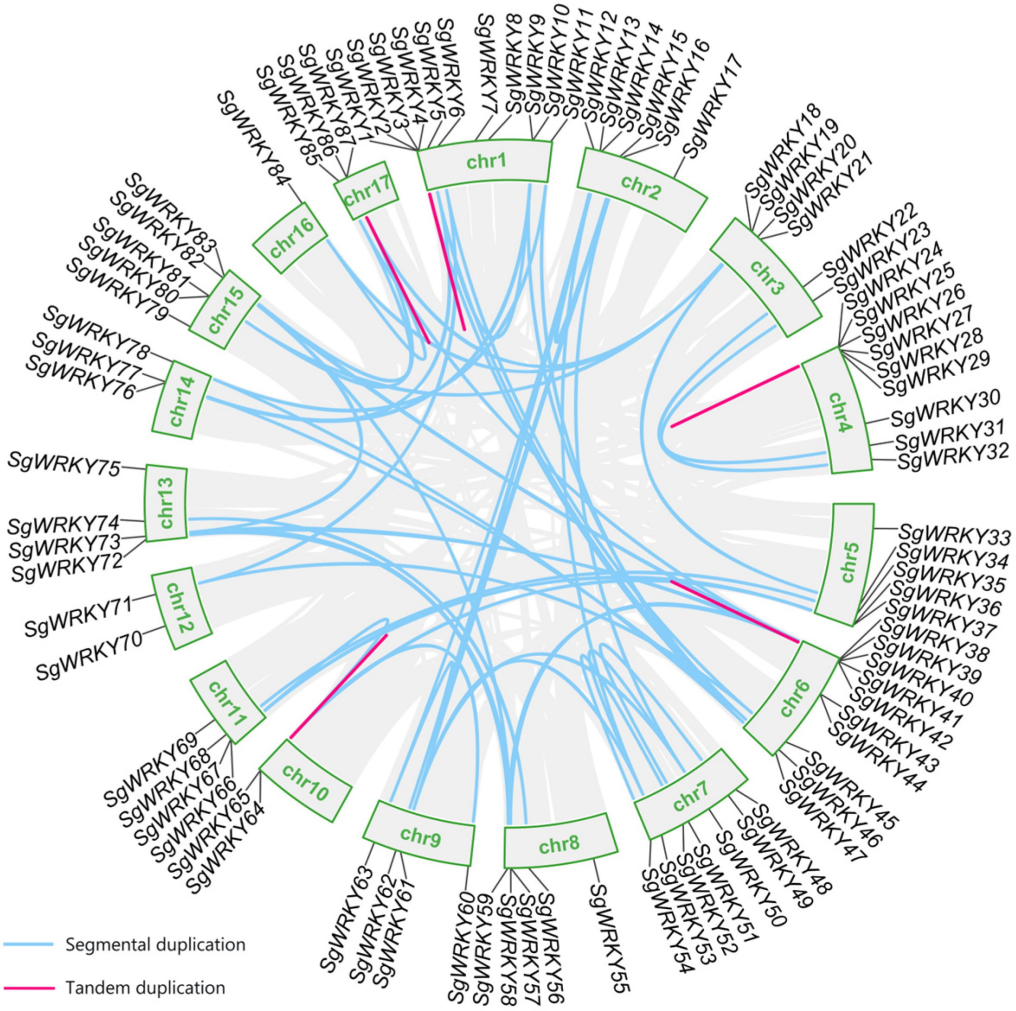


Figure 1. Chromosomal localization and collinearity analysis of 87 *SgWRKY* genes. Colored lines represent the duplicated *SgWRKY* gene pairs in the genome.

3.4. Cis-Acting Elements and Gene Ontology Analysis of SgWRKY Genes

In the promoter regions of *SgWRKY* genes, a total of 59 *cis*-acting elements were identified, excluding CAAT-box and TATA-box elements. The number of elements varied greatly. The smallest number was 9 (*SgWRKY71*), while the majority of *SgWRKY*s contained 20–30 *cis*-acting elements (Figure S4). These *cis*-acting elements mainly included abundant light-responsive motifs (MRE), hormone-related elements (ABRE, CGTCA-motif, TGA-element), abiotic stress-responsive elements (LTR, ARE), and tissue-specific developmental elements (CAT-box, AT1-motif).

In addition, we performed a GO analysis for 87 *SgWRKY* genes to predict their potential roles (Table S7). A total of 61 GO terms associated with *SgWRKY* genes in the biological process category were identified. GO terms related to biotic and abiotic stress responses included defense response to bacterium (GO:0042742), defense response to fungus (GO:0050832), response to osmotic stress (GO:0006970), and response to salt stress (GO:0009651). Other terms were associated with phytohormone signaling and plant development, such as response to salicylic acid (GO:0009751), response to jasmonic acid (GO:0009753), positive regulation of leaf senescence (GO:1900057), and floral organ senescence (GO:0080187). Focusing on the four upregulated WRKY genes (*SgWRKY24*, *84*, *67* and *77*; Figure S5), *SgWRKY84* was predicted to be associated with a broader set of annotated GO terms, which included leaf and floral organ senescence that were not found in the other three *SgWRKY* genes.



Figure 2. Multiple sequence alignment of the SgWRKY TFs. The darker purple blocks represent the WRKYGQK variant motifs. The coral pink blocks represent the C_2H_2/C_2HC motifs.

3.5. Phylogenetic, Syntenic and Selection Pressure Analysis of SgWRKY Genes Among Species

Phylogenetic analysis of 87 WRKY protein sequences aligned with 454 WRKY sequences from five other species resolved three evolutionarily conserved clades (group I-III) (Figure 3). Group II was further subdivided into five distinct subgroups (group II-a to II-e). Within group II, SgWRKYs were distributed as 7 (II-a), 8 (II-b), 25 (II-c), 7 (II-d), and 12 (II-e) (Table S8). Meanwhile, 16 SgWRKYs belonged to group I and 12 to group III. Among these groups, *S. gemmata*, *C. chekiangoleosa*, *C. lanceoleosa*, and *A. thaliana* had the highest number of group II-c WRKY proteins, followed by group I, whereas *C. oleifera* and *C. sinensis* showed the opposite pattern, with group I being the most abundant. Moreover, the number of WRKY proteins in group II-a was generally smaller, except in *C. lanceoleosa*.

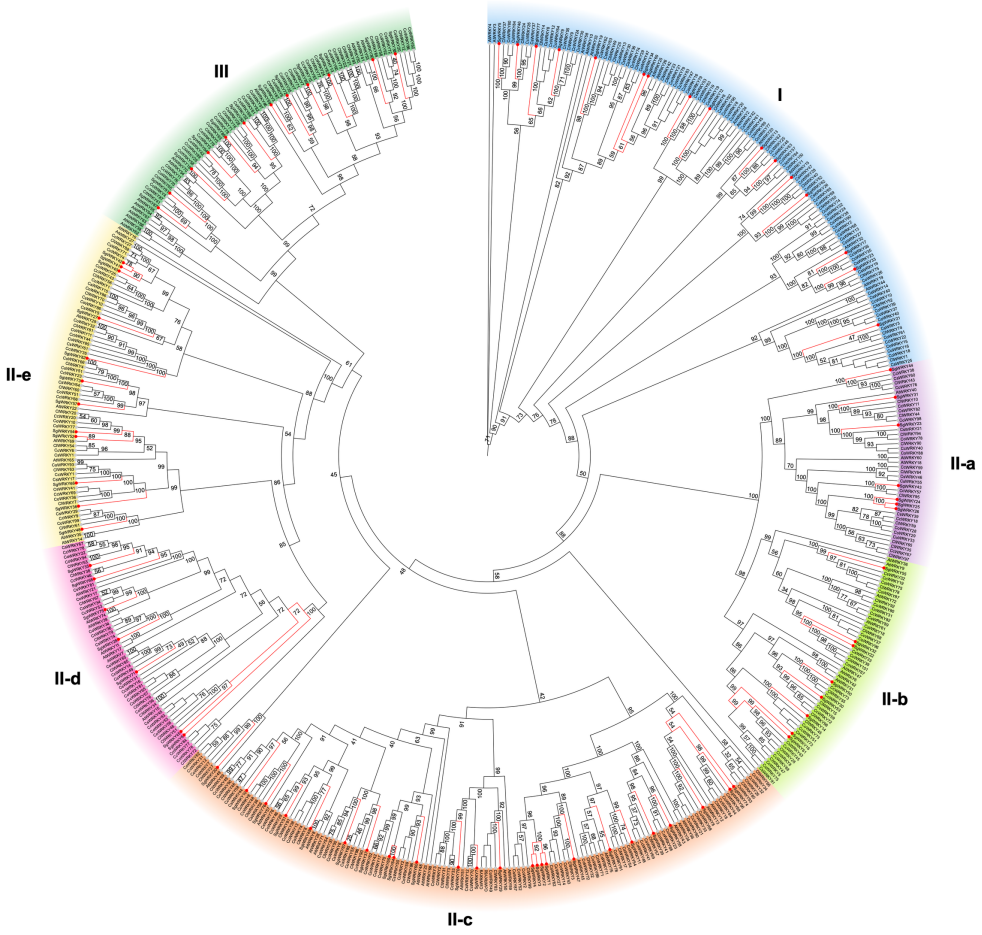


Figure 3. The maximum likelihood phylogenetic tree of the WRKY TFs in *Stewartia gemmata*, *Arabidopsis thaliana*, *Camellia chekiangoleosa*, *Camellia lanceoleosa*, *Camellia oleifera*, and *Camellia sinensis*. The red branches represent *Stewartia gemmata*. Bootstrap values are shown on each clade.

To explore *WRKY* gene family evolution within Theaceae, we also performed collinearity analyses between *S. gemmata* and five other species (Figure 4). The results revealed that more *WRKY* genes in *S. gemmata* had collinear relationships with the four other species in Theaceae than with *A. thaliana*. Specifically, 57 *SgWRKY* genes were collinear with 47 *AtWRKY* genes in *A. thaliana* (Table S9). 73 *SgWRKY*s were collinear with 43 *WRKY*s in *C. chekiangoleosa* and with 76 *WRKY*s in *C. lanceoleosa.* Similarly, 72 *SgWRKYs* were collinear with 45 *CsWRKY*s (*C. sinensis*) and 40 *CoWRKYs* (*C. oleifera*). The numbers of orthologous *WRKY* gene pairs were 89 between *S. gemmata* and *A. thaliana*, 73 between *S. gemmata* and *C. chekiangoleosa*, 196 between *S. gemmata* and *C. lanceoleosa*, 72 between *S. gemmata* and *C. oleifera*, and 72 between *S. gemmata* and *C. sinensis.* In addition, we selected *WRKY* gene

pairs of four candidate *SgWRKY*s (*SgWRKY24*, *84*, *67* and *77*) to calculate their *Ka/Ks* ratios (Table S10). The calculated results were all less than 1, indicating that these *WRKY* genes among these species were under purifying selection pressure.

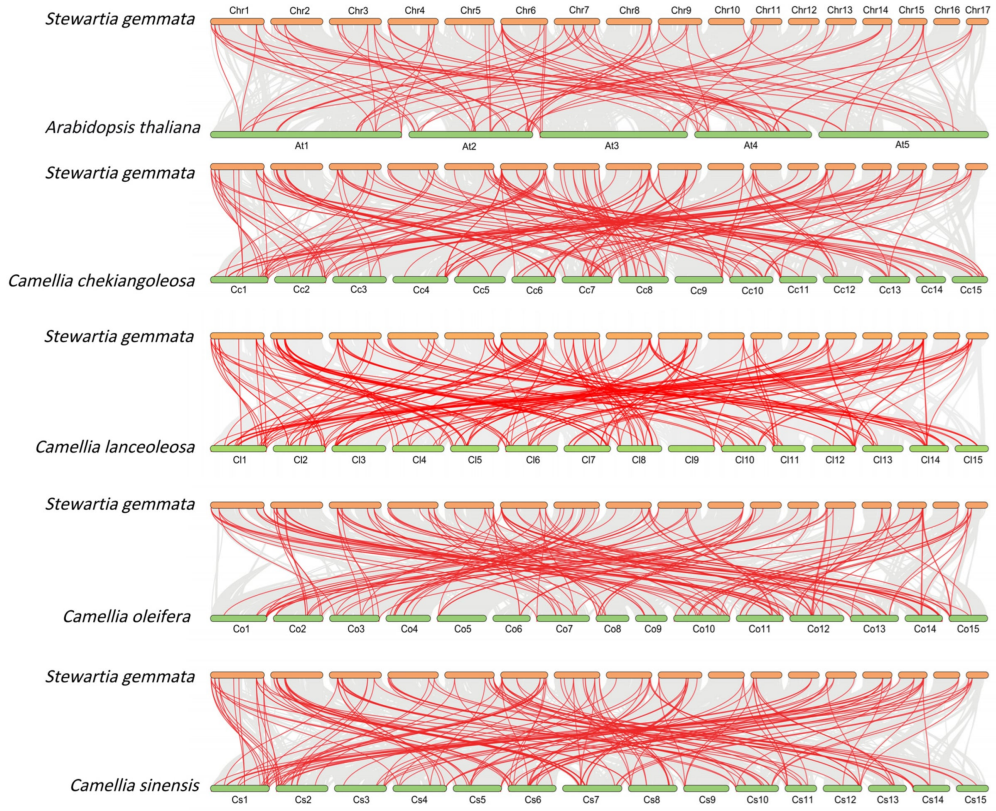


Figure 4. Synteny analysis of genes between *Stewartia gemmata* and five other species. Gray lines in the background represent the collinear blocks, while red lines represent syntenic relationships between the *WRKY* genes of *Stewartia gemmata* and their corresponding genes in five other plant genomes.

3.6. Expression Analysis of SgWRKY Gene Family

To elucidate the expression patterns of the *WRKY* gene family in *S. gemmata*, we extracted RNA from the leaves and floral organs at three different stages (54 samples in total) for transcriptome sequencing (Figure 5A). Based on transcriptome data, we conducted DEG analysis using DESeq2 with thresholds of $|\log_2 FC| > 1$ and adjusted p-value < 0.05, which showed obvious expression differences between leaves and floral organs during three flowering stages. Leaf DEG analysis revealed that 683 genes (including 3 *SgWRKY*s) were significantly upregulated from S1 to S2, 1089 genes (including 6 *SgWRKY*s) from S1 to S3, and only 128 genes (none of which were *SgWRKY*s) from S2 to S3 (Table S11), and the results were visualized as volcano plots (Figure 5B). Additionally, two *SgWRKY*s (*SgWRKY24* and *SgWRKY84*) were significantly upregulated during both the S1–S2 and S1–S3 transitions. In floral organs, 1726 genes (including 17 *SgWRKY*s) were significantly upregulated from S2 to S3, 1266 genes (including 5 *SgWRKY*s) from S1 to S3, whereas only 763 genes (none of which were *SgWRKY*s) were significantly more highly expressed in S1 than in S2 (Table S12 and Figure 5C). Notably, *SgWRKY67* and *SgWRKY77* were significantly upregulated during both the S1–S3 and S2–S3 transitions. Importantly, *SgWRKY84* was upregulated in both leaves and floral organs. In addition, more genes showed upregulated expression in floral organs than in leaves across three distinct flowering stages, reflecting tissue specificity. Consistent with the volcano plots, heatmaps based on TPM profiles (Figure 5D, Table S13) revealed the expression patterns of upregulated *SgWRKY*s across different tissues and flowering stages.

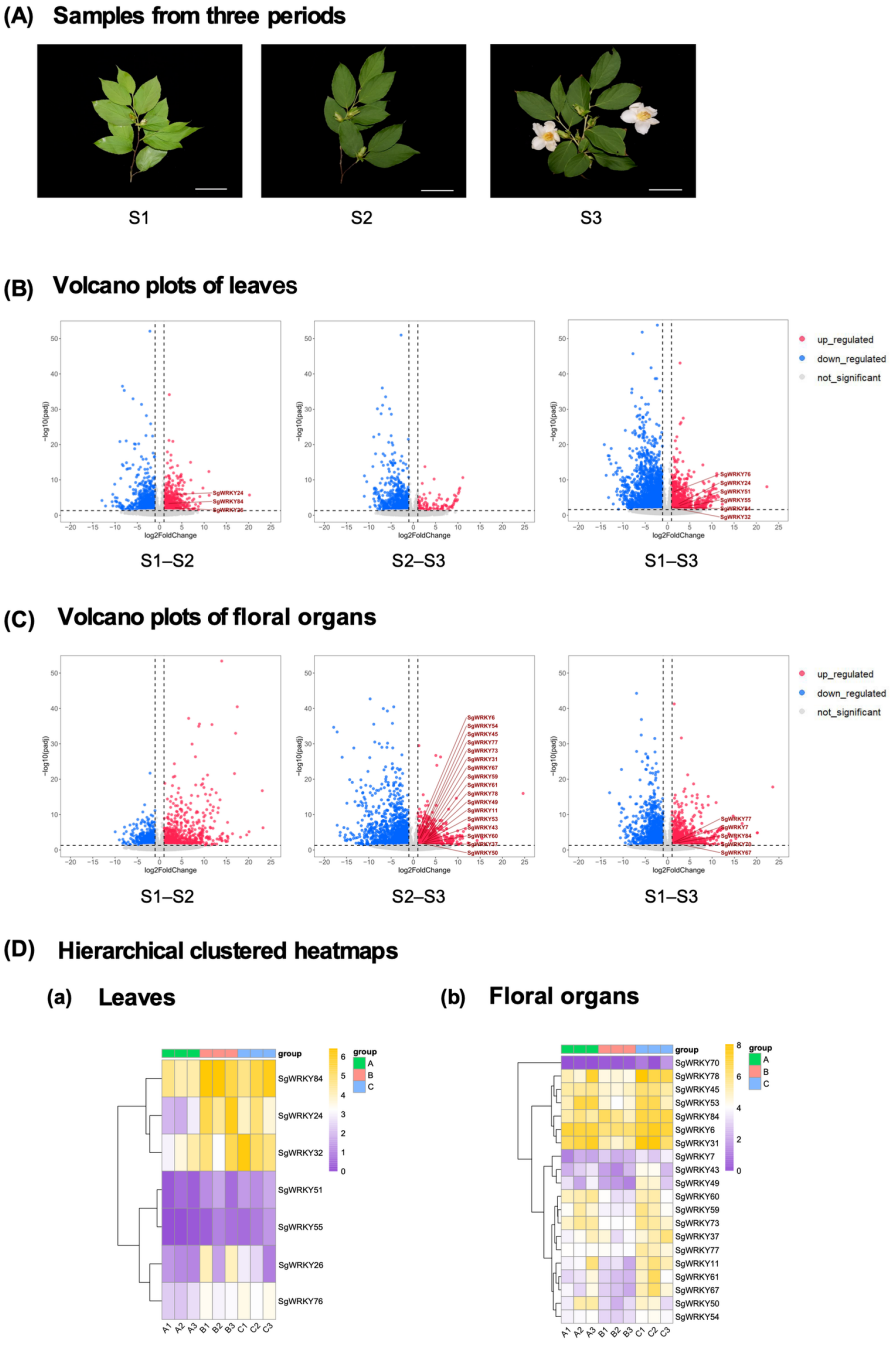


Figure 5. Morphology, differential expression, and expression profiles of *SgWRKY* genes across three flowering stages in *Stewartia gemmata*: (**A**) The morphological illustrations of *Stewartia gemmata* in three different flowering stages. Scale bar: 5 cm; (**B**) Volcano plots showing differentially expressed *SgWRKY* genes in leaves (n = 27). Red and blue dots represent significantly up-regulated and down-regulated genes, respectively (threshold: $|\log_2 FC| > 1$ and adjusted p-value < 0.05). Gray dots denote non-significant genes; (**C**) Volcano plots of *SgWRKY* genes in floral organs (n = 27), using the same filtering criteria as leaves ($|\log_2 FC| > 1$ and adjusted p-value < 0.05). Red and blue dots represent significant up- and downregulation, respectively; gray dots are non-significant; (**D**) Heatmaps showing expression profiles of *SgWRKY* genes in leaves (**a**) and floral organs (**b**) across three stages (A = S1, B = S2, C = S3). Colors represent row-scaled Z-scores, with yellow indicating higher relative expression and blue indicating lower expression. Genes were hierarchically clustered by rows based on expression similarity.

Furthermore, the qRT-PCR results were in agreement with the transcriptome predictions (Figure 6 and Table S14). One-way ANOVA and post-hoc analysis revealed that the expression of *SgWRKY24* significantly increased from S1 to S2 and from S1 to S3 ($F(2,6) = 619.2$, p-value < 0.001; post-hoc p-value < 0.001), and that *SgWRKY84* exhibited a similar trend over the same intervals ($F(2,6) = 10.61$, p-value < 0.01; post-hoc p-value < 0.05). In addition, the expression of *SgWRKY67* was significantly elevated during both S1-S3 and S2-S3 ($F(2, 6) = 164.4$, p-value < 0.001; post-hoc p-value < 0.001), and *SgWRKY77* also showed significant increases during these stages ($F(2, 6) = 14.84$, p-value = 0.005; post-hoc p-value < 0.05). Moreover, *SgWRKY24* exhibited the highest expression level at S2, and the other three *SgWRKY*s were continuously up-regulated from S1 to S3 in terms of expression trend.

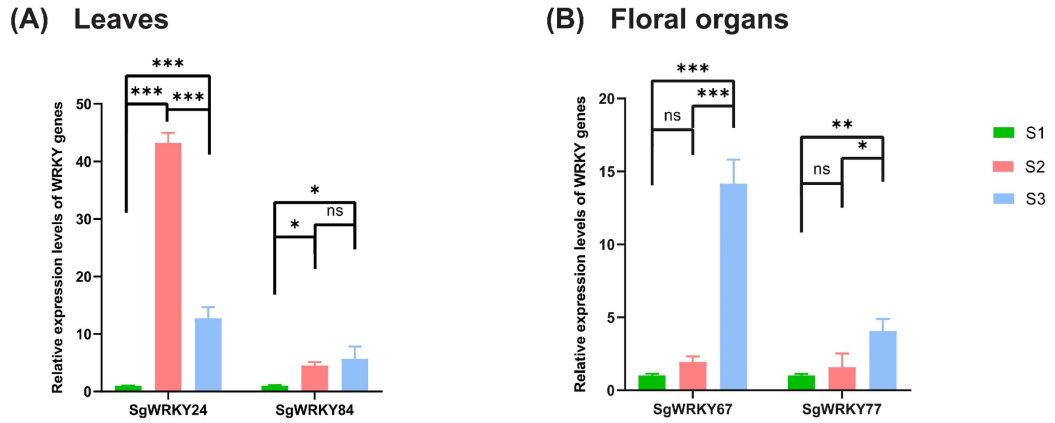


Figure 6. qRT-PCR validation of *SgWRKY* gene expression across three flowering stages (S1, S2, S3): (**A**) Expression in leaves; (**B**) Expression in floral organs. Error bars indicate standard errors of three biological replicates. Asterisks indicate statistically significant differences determined by one-way ANOVA with Tukey's post-hoc test (ns, not significant; * $p < 0.05$; ** $p < 0.01$; *** $p < 0.001$).

4. Discussion

4.1. Characterization of WRKY TFs in Stewartia gemmata

In this study, we performed a genome-wide identification and characterization of the WRKY TF family in *S. gemmata*. As summarized in the physicochemical property table of 87 SgWRKY proteins, we observed that they are universally hydrophilic, and nearly all members had an instability index over 40, consistent with the typical unstable property of plant transcription factors that enables rapid turnover in response to environmental signals. For example, MYC2 undergoes phosphorylation-coupled turnover to stimulate jasmonic acid (JA)-mediated transcriptional activity [72]. The ubiquitin E3 ligase SUBMERGENCE RESISTANT1 (SR1) from *A. thaliana* modulates submergence acclimation by regulating the stability of transcription factor WRKY33 in *Arabidopsis* [73].

Subcellular localization prediction revealed that 84 out of 87 SgWRKY proteins were targeted to the nucleus, consistent with the core function of WRKYs as nuclear transcriptional regulators [3,4]. Interestingly, three SgWRKY proteins were predicted to localize to peroxisomes (SgWRKY39, SgWRKY58) and the cytoplasm (SgWRKY64), which suggests that these SgWRKYs may play noncanonical roles, such as participating in the biosynthesis of phytohormones (e.g., jasmonic acid and salicylic acid) and being involved in plant stress responses and developmental transitions [74]. Among these proteins localized to the nucleus, only 9 SgWRKYs contained identifiable canonical NLS motifs, whereas the majority lacking predicted NLS motifs still showed nuclear localization tendency, implying these proteins may translocate into the nucleus via noncanonical transport pathways or rely on interacting partner proteins harboring functional NLS sequences [75,76].

4.2. Potential Roles of SgWRKY Genes

Cis-acting elements and GO enrichment analyses suggested that *SgWRKY* genes may be involved in plant development, hormone signaling, and stress responses. Interestingly, multiple *cis*-acting elements associated with flavonoid biosynthesis were identified in the promoters of *SgWRKY* genes, including chs-CMA1a, chs-CMA2a, chs-Unit 1 m1, and MBSI. According to the literature [77–79], *cis*-acting elements in the chalcone synthase (*CHS*) promoter are known to mediate flavonoid biosynthesis, a process closely linked to floral organ development and pigment formation in plants. The presence of these *cis*-elements suggests that SgWRKY TFs may be involved in the regulation of flavonoid accumulation in *S. gemmata*.

Phylogenetic analysis revealed that group II-c represented the largest group among all groups in *S. gemmata*, generally similar to that observed in other angiosperms [80,81]. Several studies have focused on the functions of *WRKY* gene members belonging to group II-c, particularly in biotic or abiotic stress responses and secondary metabolism regulation. Among these studies, Luan et al. discovered that overexpressing *CsWRKY50* (a group II-c member in *Cucumis sativus*) may increase the content of SA to enhance resistance to pathogen infection [82], and Kang et al. uncovered that the overexpression of *HbWRKY82* from *Hevea brasiliensis* could enhance tolerance to dehydration and salinity, while reducing sensitivity to exogenous ABA [83]. Moreover, group I *WRKY* genes were reported to participate in responses to biotic and abiotic stresses [84,85], whereas their roles in floral organ development have received considerably less attention. These findings suggest that *SgWRKY67* (group II-c) and *SgWRKY77* (group I) may play roles in stress responses and secondary metabolism. Given the crucial roles of *WRKY* genes in group II-c and group I, our findings lay the foundation for further studies on these subfamilies in *S. gemmata*.

To further explore the potential roles of these four *SgWRKY* genes, we conducted collinearity analyses between *S. gemmata* and five other species. *SgWRKY24* was found to be syntenic with *AtWRKY18* (Table S9). A previous study reported that AtWRKY18 acts as a key regulator in plant defense responses to microbial volatiles [86], implying that SgWRKY24 may play similar roles. *SgWRKY67* was found to be syntenic with *AtWRKY23*, which has been reported to participate in multiple plant developmental processes, such as regulating flavonol biosynthesis to assist auxin distribution during root development and activating *PLETHORA 3* (*PLT3*) and *PLT7* to establish callus pluripotency [87,88]. Together with its expression profile, *SgWRKY67* may play a crucial role in the development of floral organs in *S. gemmata.* Moreover, *SgWRKY77* showed a syntenic relationship with *AtWRKY3* and *AtWRKY4*. According to a previous study [89], WRKY3 and WRKY4 function as positive regulators of salt and Me-JA stress responses by modulating ROS scavenging pathways in *A. thaliana*, suggesting that *SgWRKY77* may play a conserved role in regulating stress tolerance through similar mechanisms.

In addition, we analyzed the expression patterns of *SgWRKY* genes in leaves and floral organs at different flowering stages. Through DEG analysis and qRT-PCR verification, we found that *SgWRKY24* was not continuously upregulated and instead peaked at S2 (26 April 2025). In *S. gemmata*, leaf expansion is largely completed prior to the onset of flowering (May–June) [27], suggesting that *SgWRKY24* plays a role in leaf development. The expression levels of the three genes (*SgWRKY84*, *SgWRKY67*, *SgWRKY77*) showed a progressive increase from S1 to S3, which implies that their roles might be associated with floral organ development and accumulation of flower pigments. Interestingly, DEG analysis revealed that *SgWRKY84* exhibited upregulation at S1–S3 in both leaf and floral organ tissues. Furthermore, GO enrichment analysis revealed that *SgWRKY84* was associated with terms related to leaf and floral organ senescence. These findings provide further clues for its potential role in regulating the development of leaves and floral organs.

The white flowers of *S. gemmata*, framed by green leaves and with light lemon-yellow filaments, have high ornamental value [90–92]. Further studies on *SgWRKY24, SgWRKY84*, *SgWRKY67*, and *SgWRKY77* may be worthwhile and could inform future landscaping applications. Moreover, *S. gemmata* is a deciduous species, differing from the other four Theaceae species. WRKY TFs in group III, such as AtWRKY54 and AtWRKY70, have been reported to participate in a regulatory network that modulates the progression of leaf senescence in *A. thaliana* [93]. In our study, *SgWRKY84* (belonging to group III) and *SgWRKY24* were speculated to be associated with leaf senescence based on the expression profiles. Nevertheless, no functional validations were performed in this study, and these possible associations remain untested experimentally. Additionally, environmental factors inevitably varied across the three sampling dates due to the natural field conditions. Nevertheless, all three sampled trees were adult trees derived from the same batch of seeds and grown on the same slope, ensuring a similar genetic background. Collectively, future experiments could focus on *SgWRKY84* to reveal the molecular mechanisms underlying its regulation of leaf and floral organ development, and on *SgWRKY67* to characterize its roles in biotic and abiotic stress responses and hormone signaling.

4.3. Expansion and Evolution of the WRKY Gene Family in Stewartia gemmata

The number of *SgWRKY* genes identified in *S. gemmata* is comparable to that of other Theaceae species (Table S8), suggesting that the WRKY TF family size is largely conserved within the tea family. Phylogenetic analysis revealed that group II-c contained a large number of *SgWRKY* genes. Combined with the collinearity analysis, the expansion of *SgWRKY* genes in group II-c may be due to segmental duplication (12 segmental duplications and 1 tandem duplication, Table S6). Among the *SgWRKY* gene pairs in group II-c, three pairs had a *Ka/Ks* >1, suggesting that positive selection may play roles in the functional diversification of these duplicated genes. In addition, our results showed that group I was resolved as the basal clade (Figure 3). This observation is consistent with the traditional view, which supported group I as the ancestral WRKY lineage [94,95]. This model proposes that group II and group III WRKY TFs evolved from the C-terminal WRKY domain of an ancestral group I WRKY protein, via the loss of the N-terminal WRKY domain. Consistent with our motif analysis, SgWRKY12, a group I member, appears to have lost its N-terminal WRKY domain over evolutionary time, given that it harbors only a single WRKY domain. In addition, the consistent over-representation of WRKY groups I and II-c across the six species, together with the consistently low abundance of group II-a, suggests that there is a stable evolutionary trend in WRKY group composition within this family.

To further explore the evolution of *SgWRKY* genes, we performed a synteny analysis between *S. gemmata* and other species (Table S9). Among the identified *SgWRKY* genes, *SgWRKY40, 61, 82, 83,* and *85* exhibited the largest number of WRKY gene pairs, indicating that their sequences and potential roles are highly conserved within Theaceae. Selective pressure analysis, with a particular focus on *SgWRKY24, SgWRKY84*, *SgWRKY67*, and *SgWRKY77*, was conducted to investigate whether they have undergone functional divergence (Table S10). The *Ka/Ks* ratios of the four *WRKY* genes in *S. gemmata* were all less than 1, indicating that they are under purifying selection. This suggests that *SgWRKY24, SgWRKY84*, *SgWRKY67,* and *SgWRKY77* are evolutionarily conserved across Theaceae species. Nevertheless, these results are based on bioinformatic predictions, and future functional validation is required to elucidate the precise regulatory mechanisms of these *SgWRKY* genes.

5. Conclusions

In the present study, we identified and characterized 87 *WRKY* genes in *S. gemmata* and classified them into three main groups. Our analyses revealed conserved structural features of SgWRKY TFs and suggested their potential involvement in plant development, stress adaptation, and secondary metabolism. Phylogenetic analysis showed a similar distribution pattern, with group I and group II-c containing the largest numbers of *WRKY* genes in the five Theaceae species and in *A. thaliana*. Collinearity and selection pressure analyses revealed that *SgWRKY24*, *SgWRKY84*, *SgWRKY67*, and *SgWRKY77* are evolutionarily conserved within Theaceae. In addition, these four *SgWRKY* genes were closely associated with leaf and floral organ development based on the expression profiles and GO enrichment analysis, although their functions remain to be experimentally validated. Our study lays the foundation for future functional studies aiming to reveal the molecular mechanisms by which WRKY TFs function in *S. gemmata*, a Chinese endemic deciduous tree with horticultural potential.

Supplementary Materials: The following supporting information can be downloaded at: https://www.mdpi.com/article/10.3390/horticulturae12111321/s1. Figure S1 Sequence logo of conserved WRKY domains in SgWRKY TFs; Figure S2: Conserved motifs identified in SgWRKY transcription factors; Figure S3: Neighbor-joining tree of SgWRKY transcription factors with conserved motif distributions; Figure S4: *Cis*-acting regulatory elements in the promoters of *SgWRKY* genes; Figure S5: Heatmap of GO terms for four *SgWRKY* genes; Table S1: Summary of RNA samples and sequencing data; Table S2: Gene counts at different flowering stages in different samples; Table S3: Primer sequences used for qRT-PCR validation of four *SgWRKY* genes; Table S4: Conserved domains identified in SgWRKY proteins using the NCBI CDD database; Table S5: Conserved domains identified in SgWRKY proteins using the SMART tool; Table S6: Duplicated *WRKY* gene pairs and their *Ka/Ks* ratios in *Stewartia gemmata*; Table S7: Significantly enriched GO terms (biological process) of *SgWRKY* genes; Table S8: Distribution of *WRKY* genes in six species; Table S9: Collinear *WRKY* gene pairs in six Theaceae species; Table S10: Syntenic *WRKY* gene pairs of four *SgWRKY* genes with four other Theaceae species, along with their *Ka/Ks* ratios; Table S11: Differentially expressed genes (DEGs) in leaves across flowering stages (S1, S2, S3); Table S12: Differentially expressed genes (DEGs) in floral organs across flowering stages (S1, S2, S3); Table S13: TPM matrix of transcripts in different samples across three stages (S1, S2, S3); Table S14: Quantification Cq values obtained from qRT-PCR experiments.

Author Contributions: Conceptualization, H.L.; methodology, X.Y.; software, X.Y. and F.W.; validation, X.Y.; formal analysis, X.Y. and H.L.; investigation, X.Y. and Z.Z.; resources, H.L.; data curation, X.Y.; writing—original draft preparation, X.Y. and S.H.; writing—review and editing, X.Y., J.L. and H.L.; visualization, X.Y.; supervision, H.L.; project administration, H.L.; funding acquisition, H.L. All authors have read and agreed to the published version of the manuscript.

Funding: This research was funded by the National Natural Science Foundation of China (No.32100164) and the Taizhou Science and Technology Program (No. 26nya14).

Data Availability Statement: Sequencing data are openly available in GenBank under the BioProject accession number PRJNA1502515.

Acknowledgments: The authors thank Wenhao Li for the assistance in collecting field samples.

Conflicts of Interest: The authors declare no conflicts of interest.

References

1. Harrison, S.C. A Structural Taxonomy of DNA-Binding Domains. *Nature* **1991**, *353*, 715–719. [CrossRef] [PubMed]
2. Pabo, C.O.; Sauer, R.T. Transcription Factors: Structural Families and Principles of DNA Recognition. *Annu. Rev. Biochem.* **1992**, *61*, 1053–1095. [CrossRef] [PubMed]
3. Eulgem, T.; Rushton, P.J.; Robatzek, S.; Somssich, I.E. The WRKY Superfamily of Plant Transcription Factors. *Trends Plant Sci.* **2000**, *5*, 199–206. [CrossRef] [PubMed]
4. Rushton, P.J.; Somssich, I.E.; Ringler, P.; Shen, Q.J. WRKY Transcription Factors. *Trends Plant Sci.* **2010**, *15*, 247–258. [CrossRef] [PubMed]
5. Wang, H.P.; Chen, W.Q.; Xu, Z.Y.; Chen, M.F.; Yu, D.Q. Functions of WRKYs in Plant Growth and Development. *Trends Plant Sci.* **2023**, *28*, 630–645. [CrossRef] [PubMed]
6. Ma, Z.M.; Hu, L.J. WRKY Transcription Factor Responses and Tolerance to Abiotic Stresses in Plants. *Int. J. Mol. Sci.* **2024**, *25*, 6845. [CrossRef] [PubMed]
7. Ahmad, Z.; Ramakrishnan, M.; Wang, C.Y.; Rehman, S.; Shahzad, A.; Wei, Q. Unravelling the Role of WRKY Transcription Factors in Leaf Senescence: Genetic and Molecular Insights. *J. Adv. Res.* **2025**, *74*, 191–206. [CrossRef] [PubMed]
8. Li, M.R.; Duan, Z.Q.; Zhang, S.Z.; Zhang, J.C.; Chen, J.; Song, H. The Physiological and Molecular Mechanisms of WRKY Transcription Factors Regulating Drought Tolerance: A Review. *Gene* **2025**, *938*, 149176. [CrossRef] [PubMed]
9. Long, S.L.; Jiang, J.Y.; Lin, H.Y. Whole-Genome Identification and Expression Profiles of *WRKY* Genes Related to the Leaf Expansion Period in the Camphor Tree. *Forests* **2025**, *16*, 266. [CrossRef]
10. Yang, L.; Fang, S.Y.; Liu, L.; Zhao, L.R.; Chen, W.Q.; Li, X.; Xu, Z.Y.; Chen, S.D.; Wang, H.P.; Yu, D.Q. WRKY Transcription Factors: Hubs for Regulating Plant Growth and Stress Responses. *J. Integr. Plant Biol.* **2025**, *67*, 488–509. [CrossRef] [PubMed]
11. Li, M.Y.; Shao, Y.M.; Pan, B.W.; Liu, C.; Tan, H.X. Regulation of Important Natural Products Biosynthesis by WRKY Transcription Factors in Plants. *J. Adv. Res.* **2025**, *77*, 119–135. [CrossRef] [PubMed]
12. Li, Y.Y.; Li, Z.Q.; Xu, C.Y.; Wang, Q.M. WRKYs as Regulatory Hubs of Secondary Metabolic Networks: Diverse Inducers and Distinct Responses. *Plant Commun.* **2025**, *6*, 101438. [CrossRef] [PubMed]
13. Song, H.; Cao, Y.P.; Zhao, L.G.; Zhang, J.C.; Li, S. Review: WRKY Transcription Factors: Understanding the Functional Divergence. *Plant Sci.* **2023**, *334*, 111770. [CrossRef] [PubMed]
14. Ishiguro, S.; Nakamura, K. Characterization of a cDNA Encoding a Novel DNA-Binding Protein, SPF1, That Recognizes SP8 Sequences in the 5′ Upstream Regions of Genes Coding for Sporamin and Beta-Amylase from Sweet Potato. *Mol. Gen. Genet.* **1994**, *244*, 563–571. [CrossRef] [PubMed]
15. Feng, X.; Li, G.H.; Wu, W.H.; Lyu, H.M.; Wang, J.X.; Liu, C.; Zhong, C.R.; Shi, S.H.; He, Z.W. Expansion and Adaptive Evolution of the WRKY Transcription Factor Family in *Avicennia* Mangrove Trees. *Mar. Life Sci. Technol.* **2023**, *5*, 155–168. [CrossRef] [PubMed]
16. Liu, Z.; Saiyinduleng; Chang, Q.Y.; Cheng, C.W.; Zheng, Z.M.; Yu, S. Identification of Yellowhorn (*Xanthoceras sorbifolium*) WRKY Transcription Factor Family and Analysis of Abiotic Stress Response. *Model. J. For. Res.* **2021**, *32*, 987–1004. [CrossRef]
17. Yu, X.-Q.; Gao, L.-M.; Soltis, D.E.; Soltis, P.S.; Yang, J.-B.; Fang, L.; Yang, S.-X.; Li, D.-Z. Insights into the Historical Assembly of East Asian Subtropical Evergreen Broadleaved Forests Revealed by the Temporal History of the Tea Family. *New Phytol.* **2017**, *215*, 1235–1248. [CrossRef] [PubMed]
18. Lin, H.-Y.; Sun, M.; Jin, J.-J.; Fu, C.-X.; Soltis, D.E.; Soltis, P.S.; Zhao, Y.-P. Hybridization and Incomplete Lineage Sorting Characterize the Evolutionary History of Two East Asian Clades of *Stewartia* (Theaceae). *Mol. Phylogenet. Evol.* **2026**, *214*, 108472. [CrossRef] [PubMed]
19. Wu, Z.Y.; Raven, P.H.; Hong, D.Y. *Stewartia*. In *Flora of China*; Science Press: Beijing, China, 2007; Volume 12, pp. 424–429.
20. Chien, S.S.; Cheng, W.C. *Stewartia gemmata*. *Contrib. Biol. Lab. Sci. Soc. China Bot. Ser.* **1931**, *6*, 66–69.
21. Li, J. A Systematic Study on the Genera *Stewartia* and *Hartia* (Theaceae). *Acta Phytotaxon. Sin.* **1996**, *34*, 48–67.
22. Lin, H.-Y.; Gu, K.-J.; Li, W.-H.; Zhao, Y.-P. Integrating Coalescent-Based Species Delimitation with Ecological Niche Modeling Delimited Two Species within the *Stewartia sinensis* Complex (Theaceae). *J. Syst. Evol.* **2022**, *60*, 1037–1048. [CrossRef]
23. Ai, L.J.; Wang, H.; Feng, Y.L.; Li, T.; Li, Z.Z.; Zou, M.; Zhang, Q.Y. The Healing Power of *Camellia japonica* L.: How Flower Types Influence Urban Residents' Physiological and Psychological Wellbeing. *Front. Psychol.* **2025**, *16*, 1489859. [CrossRef] [PubMed]
24. Wang, Y.P.; Zhang, R.; Zhou, Z.C. Radial Variation of Wood Anatomical Properties Determines the Demarcation of Juvenile-Mature Wood in *Schima superba*. *Forests* **2021**, *12*, 512. [CrossRef]
25. Liu, X.Y.; Li, M.Y.; Zhang, H.J.; Jiao, J.B.; Guo, X.H.; Yang, J.K.; Liu, C.J.; Guo, S.X.; Sun, Y.K.; Guo, W.H.; et al. Phenotypic Plasticity in Wild *Camellia japonica* across Climatic Zones: Responses to Variations in Soil Moisture and Light Intensity. *BMC Plant Biol.* **2025**, *25*, 1179. [CrossRef] [PubMed]
26. Wang, D.; Wang, Y.S.; Li, Z.Z.; Wang, S.; Chen, L.J. Leaf Physiological Plasticity in *Schima superba* and *Schima argentea* Is Related to Ecological Niche Width Under Varied Altitude Gradients. *Ecol. Evol.* **2025**, *15*, e71793. [CrossRef] [PubMed]
27. Li, G.Y.; Ding, B.Y. *Stewartia*. In *Flora of Zhejiang (New Edition)*; Zhejiang Science and Technology Publishing House: Hangzhou, China, 2021; Volume 3, pp. 312–315.

28. Prince, L.M.; Parks, C.R. Phylogenetic Relationships of Theaceae Inferred from Chloroplast DNA Sequence Data. *Am. J. Bot.* **2001**, *88*, 2309–2320. [CrossRef]
29. Yan, Y.J.; Davis, C.C.; Dimitrov, D.; Wang, Z.H.; Rahbek, C.; Borregaard, M.K. Phytogeographic History of the Tea Family Inferred Through High-Resolution Phylogeny and Fossils. *Syst. Biol.* **2021**, *70*, 1256–1271. [CrossRef] [PubMed]
30. Chen, W.; Hao, W.-J.; Xu, Y.-X.; Zheng, C.; Ni, D.-J.; Yao, M.-Z.; Chen, L. Isolation and Characterization of CsWRKY7, a Subgroup IId WRKY Transcription Factor from Camellia Sinensis, Linked to Development in Arabidopsis. *Int. J. Mol. Sci.* **2019**, *20*, 2815. [CrossRef] [PubMed]
31. Xiang, F.; Su, Y.; Zhou, L.Y.; Dai, C.T.; Jin, X.; Liu, H.Y.; Luo, W.G.; Yang, W.B.; Li, W. Gibberellin Promotes Theanine Synthesis by Relieving the Inhibition of CsWRKY71 on CsTSI in Tea Plant (Camellia Sinensis). *Hortic. Res.* **2025**, *12*, uhae317. [CrossRef] [PubMed]
32. Huang, D.J.; Ma, J.Q.; Chen, X.; Wang, H.J.; Tan, R.R.; Jiao, L.; Chen, J.D.; Mao, Y.X.; Chen, L. CsWRKY17 Enhances Al Accumulation by Promoting Pectin Deesterification in Tea Plant. *Hortic. Res.* **2025**, *12*, uhaf085. [CrossRef] [PubMed]
33. Chen, L.M.; Dai, H.W.; Weng, Y.W.; Zhang, K.; Zheng, S.T.; Huo, Y.B.; Yuan, L.Y.; Tong, H.R. CsWRKY51, a Novel WRKY Transcription Factor of Camellia Sinensis, Participates in Plant Architecture and Glutamine Accumulation. *Sci. Hortic.* **2025**, *341*, 113983. [CrossRef]
34. Reiser, L.; Bakker, E.; Subramaniam, S.; Chen, X.; Sawant, S.; Khosa, K.; Prithvi, T.; Berardini, T.Z. The Arabidopsis Information Resource in 2024. *GENETICS* **2024**, *227*, iyae027. [CrossRef] [PubMed]
35. Mistry, J.; Chuguransky, S.; Williams, L.; Qureshi, M.; Salazar, G.A.; Sonnhammer, E.L.L.; Tosatto, S.C.E.; Paladin, L.; Raj, S.; Richardson, L.J.; et al. Pfam: The Protein Families Database in 2021. *Nucleic Acids Res.* **2021**, *49*, D412–D419. [CrossRef] [PubMed]
36. Chen, C.J.; Wu, Y.; Li, J.W.; Wang, X.; Zeng, Z.H.; Xu, J.; Liu, Y.L.; Feng, J.T.; Chen, H.; He, Y.H.; et al. TBtools-II: A "One for All, All for One" Bioinformatics Platform for Biological Big-Data Mining. *Mol. Plant* **2023**, *16*, 1733–1742. [CrossRef] [PubMed]
37. Shen, T.-F.; Huang, B.; Xu, M.; Zhou, P.-Y.; Ni, Z.-X.; Gong, C.; Wen, Q.; Cao, F.-L.; Xu, L.-A. The Reference Genome of *Camellia chekiangoleosa* Iprovides Insights into Camellia Evolution and Tea Oil Biosynthesis. *Hortic. Res.* **2022**, *9*, uhab083. [CrossRef] [PubMed]
38. Gong, W.F.; Xiao, S.X.; Wang, L.K.; Liao, Z.Y.; Chang, Y.H.; Mo, W.J.; Hu, G.X.; Li, W.Y.; Zhao, G.; Zhu, H.G.; et al. Chromosome-level Genome of *Camellia lanceoleosa* Provides a Valuable Resource for Understanding Genome Evolution and Self-incompatibility. *Plant J.* **2022**, *110*, 881–898. [CrossRef] [PubMed]
39. Lin, P.; Wang, K.L.; Wang, Y.P.; Hu, Z.K.; Yan, C.; Huang, H.; Ma, X.J.; Cao, Y.Q.; Long, W.; Liu, W.X.; et al. The Genome of Oil-Camellia and Population Genomics Analysis Provide Insights into Seed Oil Domestication. *Genome Biol.* **2022**, *23*, 14. [CrossRef] [PubMed]
40. Zhang, X.T.; Chen, S.; Shi, L.Q.; Gong, D.P.; Zhang, S.C.; Zhao, Q.; Zhan, D.L.; Vasseur, L.; Wang, Y.B.; Yu, J.X.; et al. Haplotype-Resolved Genome Assembly Provides Insights into Evolutionary History of the Tea Plant *Camellia sinensis*. *Nat. Genet.* **2021**, *53*, 1250–1259. [CrossRef] [PubMed]
41. Gasteiger, E. ExPASy: The Proteomics Server for in-Depth Protein Knowledge and Analysis. *Nucleic Acids Res.* **2003**, *31*, 3784–3788. [CrossRef] [PubMed]
42. Horton, P.; Park, K.-J.; Obayashi, T.; Fujita, N.; Harada, H.; Adams-Collier, C.J.; Nakai, K. WoLF PSORT: Protein Localization Predictor. *Nucleic Acids Res.* **2007**, *35*, W585–W587. [CrossRef] [PubMed]
43. Almagro Armenteros, J.J.; Salvatore, M.; Emanuelsson, O.; Winther, O.; Von Heijne, G.; Elofsson, A.; Nielsen, H. Detecting Sequence Signals in Targeting Peptides Using Deep Learning. *Life Sci. Alliance* **2019**, *2*, e201900429. [CrossRef] [PubMed]
44. Nguyen Ba, A.N.; Pogoutse, A.; Provart, N.; Moses, A.M. NLStradamus: A Simple Hidden Markov Model for Nuclear Localization Signal Prediction. *BMC Bioinform.* **2009**, *10*, 202. [CrossRef] [PubMed]
45. Wang, Y.; Tang, H.; DeBarry, J.D.; Tan, X.; Li, J.; Wang, X.; Lee, T.-h.; Jin, H.; Marler, B.; Guo, H.; et al. MCScanX: A Toolkit for Detection and Evolutionary Analysis of Gene Synteny and Collinearity. *Nucleic Acids Res.* **2012**, *40*, e49. [CrossRef] [PubMed]
46. Rozas, J.; Ferrer-Mata, A.; Sánchez-DelBarrio, J.C.; Guirao-Rico, S.; Librado, P.; Ramos-Onsins, S.E.; Sánchez-Gracia, A. DnaSP 6: DNA Sequence Polymorphism Analysis of Large Data Sets. *Mol. Biol. Evol.* **2017**, *34*, 3299–3302. [CrossRef] [PubMed]
47. Kumar, S.; Stecher, G.; Suleski, M.; Sanderford, M.; Sharma, S.; Tamura, K. MEGA12: Molecular Evolutionary Genetic Analysis Version 12 for Adaptive and Green Computing. *Mol. Biol. Evol.* **2024**, *41*, msae263. [CrossRef] [PubMed]
48. Marchler-Bauer, A. CDD: A Conserved Domain Database for Protein Classification. *Nucleic Acids Res.* **2005**, *33*, D192–D196. [CrossRef] [PubMed]
49. Madeira, F.; Madhusoodanan, N.; Lee, J.; Eusebi, A.; Niewielska, A.; Tivey, A.R.N.; Lopez, R.; Butcher, S. The EMBL-EBI Job Dispatcher Sequence Analysis Tools Framework in 2024. *Nucleic Acids Res.* **2024**, *52*, W521–W525. [CrossRef] [PubMed]
50. Waterhouse, A.M.; Procter, J.B.; Martin, D.M.A.; Clamp, M.; Barton, G.J. Jalview Version 2—A Multiple Sequence Alignment Editor and Analysis Workbench. *Bioinformatics* **2009**, *25*, 1189–1191. [CrossRef] [PubMed]
51. Crooks, G.E.; Hon, G.; Chandonia, J.-M.; Brenner, S.E. WebLogo: A Sequence Logo Generator. *Genome Res.* **2004**, *14*, 1188–1190. [CrossRef] [PubMed]

52. Bailey, T.L.; Johnson, J.; Grant, C.E.; Noble, W.S. The MEME Suite. *Nucleic Acids Res.* **2015**, *43*, W39–W49. [CrossRef] [PubMed]
53. Xie, J.M.; Chen, Y.R.; Cai, G.J.; Cai, R.L.; Hu, Z.; Wang, H. Tree Visualization By One Table (tvBOT): A Web Application for Visualizing, Modifying and Annotating Phylogenetic Trees. *Nucleic Acids Res.* **2023**, *51*, W587–W592. [CrossRef] [PubMed]
54. Lescot, M. PlantCARE, a Database of Plant *Cis*-Acting Regulatory Elements and a Portal to Tools for in Silico Analysis of Promoter Sequences. *Nucleic Acids Res.* **2002**, *30*, 325–327. [CrossRef] [PubMed]
55. Bu, D.C.; Luo, H.T.; Huo, P.P.; Wang, Z.H.; Zhang, S.; He, Z.H.; Wu, Y.; Zhao, L.H.; Liu, J.J.; Guo, J.C.; et al. KOBAS-i: Intelligent Prioritization and Exploratory Visualization of Biological Functions for Gene Enrichment Analysis. *Nucleic Acids Res.* **2021**, *49*, W317–W325. [CrossRef] [PubMed]
56. Katoh, K.; Standley, D.M. MAFFT Multiple Sequence Alignment Software Version 7: Improvements in Performance and Usability. *Mol. Biol. Evol.* **2013**, *30*, 772–780. [CrossRef] [PubMed]
57. Capella-Gutiérrez, S.; Silla-Martínez, J.M.; Gabaldón, T. trimAl: A Tool for Automated Alignment Trimming in Large-Scale Phylogenetic Analyses. *Bioinformatics* **2009**, *25*, 1972–1973. [CrossRef] [PubMed]
58. Minh, B.Q.; Schmidt, H.A.; Chernomor, O.; Schrempf, D.; Woodhams, M.D.; Von Haeseler, A.; Lanfear, R. IQ-TREE 2: New Models and Efficient Methods for Phylogenetic Inference in the Genomic Era. *Mol. Biol. Evol.* **2020**, *37*, 1530–1534. [CrossRef] [PubMed]
59. Hoang, D.T.; Chernomor, O.; Von Haeseler, A.; Minh, B.Q.; Vinh, L.S. UFBoot2: Improving the Ultrafast Bootstrap Approximation. *Mol. Biol. Evol.* **2018**, *35*, 518–522. [CrossRef] [PubMed]
60. Kalyaanamoorthy, S.; Minh, B.Q.; Wong, T.K.F.; Von Haeseler, A.; Jermiin, L.S. ModelFinder: Fast Model Selection for Accurate Phylogenetic Estimates. *Nat. Methods* **2017**, *14*, 587–589. [CrossRef] [PubMed]
61. Schroeder, A.; Mueller, O.; Stocker, S.; Salowsky, R.; Leiber, M.; Gassmann, M.; Lightfoot, S.; Menzel, W.; Granzow, M.; Ragg, T. The RIN: An RNA Integrity Number for Assigning Integrity Values to RNA Measurements. *BMC Mol. Biol.* **2006**, *7*, 3. [CrossRef] [PubMed]
62. Kim, D.; Paggi, J.M.; Park, C.; Bennett, C.; Salzberg, S.L. Graph-Based Genome Alignment and Genotyping with HISAT2 and HISAT-Genotype. *Nat. Biotechnol.* **2019**, *37*, 907–915. [CrossRef] [PubMed]
63. Pertea, M.; Kim, D.; Pertea, G.M.; Leek, J.T.; Salzberg, S.L. Transcript-Level Expression Analysis of RNA-Seq Experiments with HISAT, StringTie and Ballgown. *Nat. Protoc.* **2016**, *11*, 1650–1667. [CrossRef] [PubMed]
64. Love, M.I.; Huber, W.; Anders, S. Moderated Estimation of Fold Change and Dispersion for RNA-Seq Data with DESeq2. *Genome Biol.* **2014**, *15*, 550. [CrossRef] [PubMed]
65. Wickham, H. *Ggplot2: Elegant Graphics for Data Analysis*, 2nd ed.; Springer: Berlin/Heidelberg, Germany, 2016.
66. Wong, M.L.; Medrano, J.F. Real-Time PCR for mRNA Quantitation. *BioTechniques* **2005**, *39*, 75–85. [CrossRef] [PubMed]
67. Wu, Z.-J.; Li, X.-H.; Liu, Z.-W.; Li, H.; Wang, Y.-X.; Zhuang, J. Transcriptome-Wide Identification of *Camellia sinensis* WRKY Transcription Factors in Response to Temperature Stress. *Mol. Genet. Genom.* **2016**, *291*, 255–269. [CrossRef] [PubMed]
68. Xu, W.; Dong, Y.; Yu, Y.; Xing, Y.; Li, X.; Zhang, X.; Hou, X.; Sun, X. Identification and Evaluation of Reliable Reference Genes for Quantitative Real-Time PCR Analysis in Tea Plants under Differential Biotic Stresses. *Sci. Rep.* **2020**, *10*, 2429. [CrossRef] [PubMed]
69. Koressaar, T.; Remm, M. Enhancements and Modifications of Primer Design Program Primer3. *Bioinformatics* **2007**, *23*, 1289–1291. [CrossRef] [PubMed]
70. Untergasser, A.; Cutcutache, I.; Koressaar, T.; Ye, J.; Faircloth, B.C.; Remm, M.; Rozen, S.G. Primer3—New Capabilities and Interfaces. *Nucleic Acids Res.* **2012**, *40*, e115. [CrossRef] [PubMed]
71. Schmittgen, T.D.; Livak, K.J. Analyzing Real-Time PCR Data by the Comparative CT Method. *Nat. Protoc.* **2008**, *3*, 1101–1108. [CrossRef] [PubMed]
72. Zhai, Q.Z.; Yan, L.H.; Tan, D.; Chen, R.; Sun, J.Q.; Gao, L.Y.; Dong, M.-Q.; Wang, Y.C.; Li, C.Y. Phosphorylation-Coupled Proteolysis of the Transcription Factor MYC2 Is Important for Jasmonate-Signaled Plant Immunity. *PLoS Genet.* **2013**, *9*, e1003422. [CrossRef] [PubMed]
73. Liu, B.; Jiang, Y.Z.; Tang, H.; Tong, S.F.; Lou, S.L.; Shao, C.; Zhang, J.L.; Song, Y.; Chen, N.N.; Bi, H.; et al. The Ubiquitin E3 Ligase SR1 Modulates the Submergence Response by Degrading Phosphorylated WRKY33 in *Arabidopsis*. *Plant Cell* **2021**, *33*, 1771–1789. [CrossRef] [PubMed]
74. Molina-Moya, E.; Rodríguez-González, A.; Peláez-Vico, M.A.; Sandalio, L.M.; Romero-Puertas, M.C. Peroxisomal-Dependent Signalling and Dynamics Modulate Plant Stress Responses: Reactive Oxygen and Nitrogen Species as Key Molecules. *J. Exp. Bot.* **2025**, *76*, 3706–3721. [CrossRef] [PubMed]
75. Hackenberg, D.; Wu, Y.; Voigt, A.; Adams, R.; Schramm, P.; Grimm, B. Studies on Differential Nuclear Translocation Mechanism and Assembly of the Three Subunits of the *Arabidopsis thaliana* Transcription Factor NF-Y. *Mol. Plant* **2012**, *5*, 876–888. [CrossRef] [PubMed]
76. Marathe, S.; Grotewold, E.; Otegui, M.S. Should I Stay or Should I Go? Trafficking of Plant Extra-Nuclear Transcription Factors. *Plant Cell* **2024**, *36*, 1524–1539. [CrossRef] [PubMed]

77. Pollak, P.E.; Vogt, T.; Mo, Y.; Taylor, L.P. Chalcone Synthase and Flavonol Accumulation in Stigmas and Anthers of Petunia Hybrida. *Plant Physiol.* **1993**, *102*, 925–932. [CrossRef] [PubMed]
78. Liu, Y.L.; Lou, Q.; Xu, W.R.; Xin, Y.; Bassett, C.; Wang, Y.J. Characterization of a Chalcone Synthase (CHS) Flower-Specific Promoter from Lilium Orential 'Sorbonne'. *Plant Cell Rep.* **2011**, *30*, 2187–2194. [CrossRef] [PubMed]
79. Chen, G.Q.; He, W.Z.; Guo, X.X.; Pan, J.S. Genome-Wide Identification, Classification and Expression Analysis of the MYB Transcription Factor Family in *Petunia*. *Int. J. Mol. Sci.* **2021**, *22*, 4838. [CrossRef] [PubMed]
80. Schluttenhofer, C.; Pattanaik, S.; Patra, B.; Yuan, L. Analyses of *Catharanthus roseu*s and *Arabidopsis thaliana* WRKY Transcription Factors Reveal Involvement in Jasmonate Signaling. *BMC Genom.* **2014**, *15*, 502. [CrossRef] [PubMed]
81. Wang, M.; Vannozzi, A.; Wang, G.; Liang, Y.-H.; Tornielli, G.B.; Zenoni, S.; Cavallini, E.; Pezzotti, M.; Cheng, Z.-M. Genome and Transcriptome Analysis of the Grapevine (*Vitis vinifera* L.) WRKY Gene Family. *Hortic. Res.* **2014**, *1*, 14016. [CrossRef] [PubMed]
82. Luan, Q.Q.; Chen, C.H.; Liu, M.Y.; Li, Q.; Wang, L.N.; Ren, Z.H. *CsWRKY50* Mediates Defense Responses to *Pseudoperonospora cubensis* Infection in *Cucumis sativus*. *Plant Sci.* **2019**, *279*, 59–69. [CrossRef] [PubMed]
83. Kang, G.J.; Yan, D.; Chen, X.L.; Yang, L.F.; Zeng, R.Z. HbWRKY82, a Novel IIc WRKY Transcription Factor from *Hevea brasiliensis* Associated with Abiotic Stress Tolerance and Leaf Senescence in *Arabidopsis*. *Physiol. Plant.* **2021**, *171*, 151–160. [CrossRef] [PubMed]
84. Liu, X.F.; Song, Y.Z.; Xing, F.Y.; Wang, N.; Wen, F.J.; Zhu, C.X. *GhWRKY25*, a Group I *WRKY* Gene from Cotton, Confers Differential Tolerance to Abiotic and Biotic Stresses in Transgenic *Nicotiana benthamiana*. *Protoplasma* **2016**, *253*, 1265–1281. [CrossRef] [PubMed]
85. Lv, M.C.; Luo, W.; Ge, M.M.; Guan, Y.J.; Tang, Y.; Chen, W.M.; Lv, J.Y. A Group I WRKY Gene, *TaWRKY133*, Negatively Regulates Drought Resistance in Transgenic Plants. *Int. J. Mol. Sci.* **2022**, *23*, 12026. [CrossRef] [PubMed]
86. Wenke, K.; Wanke, D.; Kilian, J.; Berendzen, K.; Harter, K.; Piechulla, B. Volatiles of Two Growth-inhibiting Rhizobacteria Commonly Engage AtWRKY18 Function. *Plant J.* **2012**, *70*, 445–459. [CrossRef] [PubMed]
87. Grunewald, W.; De Smet, I.; Lewis, D.R.; Löfke, C.; Jansen, L.; Goeminne, G.; Vanden Bossche, R.; Karimi, M.; De Rybel, B.; Vanholme, B.; et al. Transcription Factor WRKY23 Assists Auxin Distribution Patterns during *Arabidopsis* Root Development through Local Control on Flavonol Biosynthesis. *Proc. Natl. Acad. Sci. USA* **2012**, *109*, 1554–1559. [CrossRef] [PubMed]
88. Xu, C.Y.; Chang, P.J.; Guo, S.Q.; Yang, X.N.; Liu, X.C.; Sui, B.F.; Yu, D.X.; Xin, W.; Hu, Y.X. Transcriptional Activation by WRKY23 and Derepression by Removal of bHLH041 Coordinately Establish Callus Pluripotency in *Arabidopsis* Regeneration. *Plant Cell* **2023**, *36*, 158–173. [CrossRef] [PubMed]
89. Li, P.; Li, X.W.; Jiang, M. CRISPR/Cas9-Mediated Mutagenesis of *WRKY3* and *WRKY4* Function Decreases Salt and Me-JA Stress Tolerance in *Arabidopsis thaliana*. *Mol. Biol. Rep.* **2021**, *48*, 5821–5832. [CrossRef] [PubMed]
90. Spongberg, S.A.; Fordham, A.J. Stewartias-Small Trees and Shrubs for All Seasons. *Arnoldia* **1975**, *35*, 165–180. [CrossRef]
91. Hsu, E.; Boland, T.; Camelbeke, K. *Stewartia* in Cultivation. *Plantsman (New Ser.)* **2008**, *7*, 78–87. [CrossRef] [PubMed]
92. Del Tredici, P. Chinese Stewartia *Stewartia sinensis*. *Arnoldia* **2010**, *68*, 59–60. [CrossRef]
93. Besseau, S.; Li, J.; Palva, E.T. WRKY54 and WRKY70 Co-Operate as Negative Regulators of Leaf Senescence in *Arabidopsis thaliana*. *J. Exp. Bot.* **2012**, *63*, 2667–2679. [CrossRef] [PubMed]
94. Zhang, Y.J.; Wang, L.J. The WRKY Transcription Factor Superfamily: Its Origin in Eukaryotes and Expansion in Plants. *BMC Evol. Biol.* **2005**, *5*, 1. [CrossRef] [PubMed]
95. Rinerson, C.I.; Rabara, R.C.; Tripathi, P.; Shen, Q.J.; Rushton, P.J. The Evolution of WRKY Transcription Factors. *BMC Plant Biol.* **2015**, *15*, 66. [CrossRef] [PubMed]

Disclaimer/Publisher's Note: The statements, opinions and data contained in all publications are solely those of the individual author(s) and contributor(s) and not of MDPI and/or the editor(s). MDPI and/or the editor(s) disclaim responsibility for any injury to people or property resulting from any ideas, methods, instructions or products referred to in the content.